NeuroImage 56 (2011) 744–752

Contents lists available at ScienceDirect

NeuroImage

journal homepage: www.elsevier.com/locate/ynimg

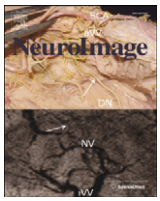

Multi-voxel coding of stimuli, rules, and responses in human frontoparietal cortex

Alexandra Woolgar *, Russell Thompson, Daniel Bor, John Duncan

MRC Cognition and Brain Sciences Unit, 15 Chaucer Road, Cambridge, CB2 7EF, UK

ARTICLE INFO

Article history:
Received 6 November 2009
Revised 17 March 2010
Accepted 14 April 2010
Available online 18 April 2010

ABSTRACT

In human functional magnetic resonance imaging (fMRI), a characteristic pattern of frontal and parietal activity is produced by many different cognitive demands. Although frontoparietal cortex has been shown to represent a variety of task features in different contexts, little is known about detailed representation of different task features within and across different regions. We used multi-voxel pattern analysis (MVPA) of human fMRI data to assess the representational content of frontoparietal cortex in a simple stimulus–response task. Stimulus–response mapping rule was the most strongly represented task feature, significantly coded in a lateral frontal region surrounding the inferior frontal sulcus, a more ventral region including the anterior insula/frontal operculum, and the intraparietal sulcus. Next strongest was coding of the instruction cue (screen color) indicating which rule should be applied. Coding of individual stimuli and responses was weaker, approaching significance in a subset of regions. In line with recent single unit data, the results show a broad representation of task-relevant information across human frontoparietal cortex, with strong representation of a general rule or cognitive context, and weaker coding of individual stimulus/response instances.

Introduction

Frontoparietal cortex is important in diverse forms of behavior. In human studies using functional magnetic resonance imaging (fMRI), a characteristic pattern of frontoparietal activity is produced by many different kinds of cognitive activity, including perceptual discrimination, resolution of response conflict, working memory storage/manipulation and episodic memory encoding/retrieval (Duncan and Owen, 2000; Nyberg et al., 2003; Dosenbach et al., 2006; Duncan, 2006). The pattern incorporates the cortex around the inferior frontal sulcus (IFS), the anterior insula/frontal operculum (AI/FO), the dorsal anterior cingulate/pre-supplementary motor area (ACC/pre-SMA), and the intraparietal sulcus (IPS). Given its generality, we have called this the multiple-demand or MD pattern (Duncan, 2006).

It is widely accepted that frontoparietal cortex is important in high-level cognitive control. One proposal is that such control is exerted by selective coding of task-relevant information. This selective frontoparietal representation may serve as a source of bias to other brain systems, supporting related information processing (Desimone and Duncan, 1995; Dehaene et al., 1998; Miller and Cohen, 2001). Several strands of evidence suggest that MD regions can represent many different kinds of task-relevant information. In monkey studies, the activity of frontal and parietal cells codes various task features, including stimuli, responses, rules and rewards (e.g. Niki and Watanabe, 1976; Andersen et al., 1985; Sakagami and Niki, 1994; Snyder et al., 1997; Asaad et al., 1998; Hoshi et al., 1998; White and Wise, 1999; Wallis et al., 2001; Stoet and Snyder, 2004; Gail and Andersen, 2006; Sigala et al., 2008).

In conventional fMRI the representational content of MD regions has been more difficult to determine, but the question can be examined through multi-voxel pattern analysis (MVPA). In MVPA, information coding is demonstrated by differences in the voxelwise pattern of activity evoked by different events such as different visual stimuli or different motor outputs (Haynes and Rees, 2006). Such differences might arise through variation across voxels in the proportion of neurons responding to different task events. In agreement with the monkey literature, recent work using MVPA suggests that human frontoparietal cortex can code a range of different types of information, including the task-relevant features of moving dot figures (Li et al., 2007), and more abstract task features such as intended mathematical operation (Haynes et al., 2007). In the current study, we used MVPA to assess the representational content of MD regions during a simple visual stimulus–response task. Both in specific MD regions of interest and across the whole brain, we examined coding of rules for transforming stimuli into responses, and coding of individual stimulus-response alternatives.

On the one hand, we predicted broad coding of different task features across MD regions. On the other, we wished to compare task features for their relative strength of coding. The question is illustrated by a recent single unit study of monkey prefrontal cortex (Sigala et al., 2008). In this study, a cue at trial onset indicated the target picture for the current trial; the monkey then watched a series of pictures and responded after the target appeared. Analyzing the pattern of activity across a

* Corresponding author. Fax: +44 1223 359062.
E-mail address: Alexandra.woolgar@mrc-cbu.cam.ac.uk (A. Woolgar).

1053-8119/$ – see front matter © 2010 Elsevier Inc. All rights reserved.
doi:10.1016/j.neuroimage.2010.04.035

population of prefrontal cells, the authors asked how dissimilar activity patterns were for different task events. They found good discrimination between different task phases (cue, delay, and target), corresponding to different cognitive operations required in the different stages of the task, and weaker discrimination of stimulus identity within each phase. In our study, analogously, we compared coding of a general stimulus–response mapping rule with coding of specific stimulus and response identities.

Materials and methods

Participants

Seventeen participants (nine female, mean age = 21.6, SD = 4.12) took part in this study and were reimbursed for their time. Participants were right handed and had normal or corrected to normal vision. All participants gave written informed consent to take part. The study was approved by the Hertfordshire Local Research Ethics Committee.

Task design

On each trial the stimulus was a blue square measuring approximately 2 × 2° presented on a projector and viewed through a head-coil-mounted mirror in the scanner. It could appear in one of four positions, indicated on the screen by four place holders. Place holders were white squares with a black outline (2 × 2°), arranged in a horizontal row in the center of the screen and separated by approximately 1° edge to edge. Participants responded by pressing one of four response keys using index and middle fingers from each hand.

There were two incompatible stimulus–response mappings between the four stimulus positions and the four response keys (Fig. 1). The current rule to use was indicated by the background color of the screen with two colors indicating each rule: blue and yellow indicated rule one, and pink and green indicated rule two.

Participants learnt the rules and corresponding background colors outside the scanner (rule 1 first) and practiced a mixture of the two rules for approximately 10 min. They were instructed to respond as quickly as possible without making any mistakes, and were shown feedback (number of trials completed and percentage correct) after each block of trials.

Acquisition

FMRI data were acquired using a Siemens 3 T TimTrio scanner with a 12 channel head coil. We used a sequential descending T2*-weighted echo planar imaging (EPI) acquisition sequence with the following parameters: acquisition time 2000 ms; echo time 30 ms; 32 oblique axial slices with a slice thickness of 3.0 mm and a 0.75 mm inter-slice gap; in plane resolution 3.0 × 3.0 mm; matrix 64 × 64; field of view 192 mm; flip angle 78°. T1-weighted MPRAGE structural images were also acquired for all participants (slice thickness 1.0 mm, resolution 1.0 × 1.0 × 1.5 mm, field of view 256 mm, 160 slices).

We used an event related fMRI design in which the 16 stimuli (four positions * four background colors) were presented in random order. Stimuli remained visible until the participant responded. There was an interval of 1000 ms between response and display of the subsequent stimulus, during which the placeholders were visible against a white background. Participants completed two runs of trials in a single scanning session. Each run consisted of five short blocks of trials, lasting 3 min each, with a 30 s gap between blocks. The total EPI time was 34 min.

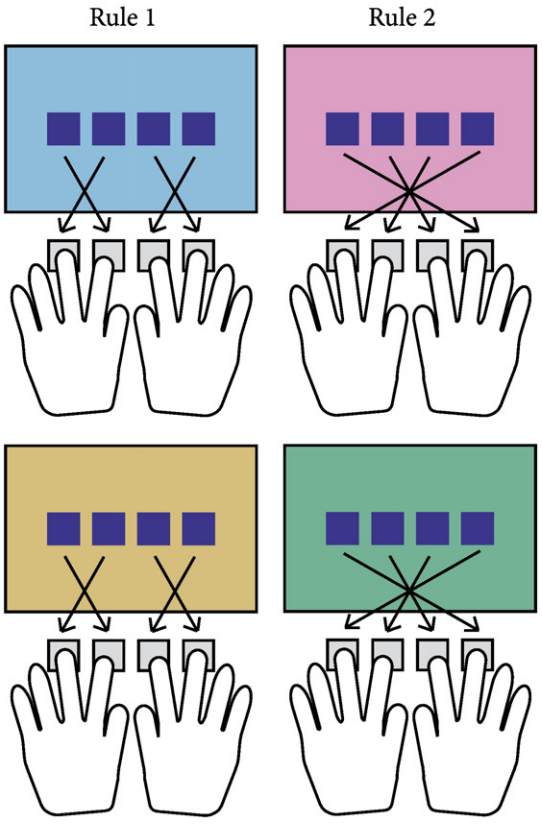

Fig. 1. There were two incompatible stimulus–response mappings between the four stimulus positions and the four response keys. The background color of the screen indicated which rule to use on the current trial: blue and yellow indicated rule one and pink and green indicated rule two. Participants responded with the index and middle finger of each hand.

Analysis

Analyses examined four task features: rule, stimulus position, response, and background color. Since position and response were partially confounded in our design, we compared inner with outer positions (which have equal contributions from each of the four responses and each of the two rules) and inner with outer responses (which have equal contributions from each of the four stimulus positions, each of the two hands, and each of the two rules). Background colors were always compared within rule. Conventional univariate analyses examined differences in overall activation evoked by different rules, positions, responses, and colors. Multi-voxel pattern analysis (MVPA) was used to discriminate fine grained activation patterns associated with different positions, responses, rules and colors. As the central aim of the current study was to investigate the representational content of MD cortex, the main analyses focused on prefrontal and parietal regions of interest (see below). Whole brain analyses were also carried out using a searchlight method in order to identify any additional regions showing task-relevant feature coding.

Pre-processing

Image realignment, slice timing correction and co-registration to structural images was carried out using Automatic Analysis version 2.0 for SPM5 (http://imaging.mrc-cbu.cam.ac.uk/imaging/AutomaticAnalysisIntroduction). For univariate analyses, data were additionally normalized using a segment and normalize routine (simultaneous grey/white matter segment and normalize) and smoothed (10 mm FWHM Gaussian kernel) using the same software. In all cases data were high pass filtered (128 s).

Regions of interest (ROIs)

MD ROIs were defined using data from a prior review of activity associated with a diverse set of cognitive demands (Duncan and Owen, 2000). We used the kernel method described in Cusack et al. (2010). To ensure symmetrical ROIs, all peaks from the original review were first projected onto a single hemisphere. A point was placed at the location of each peak and the resulting image was smoothed (15 mm FWHM Gaussian kernel) and thresholded at 3.5 times the height of a single peak. The resulting regions were then reflected onto the opposite hemisphere. A plane at the local minimum was used to divide lateral prefrontal regions into a more dorsal part, in and around the IFS, and a more ventral part, focused around the AI/FO. The two left and right medial ROIs abutting each other at the midline were unified into a single ACC/pre-SMA region. The procedure yielded a total of seven ROIs (Fig. 2): left and right IFS (centre of mass +/− 38 26 24, volume 17000 mm^3); left and right AI/FO (+/−35 19 3, 3000 mm^3); left and right IPS (+/−35 −58 41, 7000 mm^3) and ACC/pre-SMA (0 23 39, 21000 mm^3). Four further ROIs were taken from the Brodmann template provided with MRIcro (Rorden and Brett, 2000): left and right visual cortex (BA 17/18, centre of mass −13 −81 3, 16 −79 3, volume 54000 mm^3) and left and right motor cortex (BA 4, −27 −23 60, 28 −23 60, 18000 mm^3). All co-ordinates are given in MNI152 space (McConnell Brain Imaging Centre, Montreal Neurological Institute).

Univariate analyses

The univariate effects of rule, position, response, and color were analyzed using the multiple regression approach of SPM5 (Wellcome Department of Imaging Neuroscience, London, UK; www.fil.ion.ucl.ac.uk). For each participant, beta values for the four stimulus positions, four responses and four background colors were estimated in each of the ten blocks. Movement parameters, block means, and run means were included as covariates of no interest. Trials were modeled as epochs lasting from stimulus onset until response, and each trial contributed to the estimation of three betas (one stimulus position, one response, and one background color). Error trials were excluded from the analysis.

ROI analyses were carried out using the MarsBar toolbox for SPM5 (Brett et al., 2002). For each region, a mean time course was calculated across voxels and effect sizes were estimated using the model described above. Effect sizes for each participant were then used in a series of group analyses. For the IFS, AI/FO and IPS ROIs, each task feature was analyzed using a separate two-way repeated measures analysis of variance (ANOVA), with task feature (e.g. rule) and hemisphere as factors. Since the ACC/pre-SMA ROI was bilateral, data from this ROI were entered into a one-way ANOVA comparable to the one-sample *t*-tests used in the whole brain analysis. To account for the four statistical tests that were carried out for each task feature, we evaluated the results using a Bonferroni adjusted significance threshold of $p = 0.0125$. The two additional ROIs (BA 4 and BA 17/18) were analyzed in the same way. Since we had strong a priori hypotheses in these regions, we did not adjust our significance threshold for these tests.

For whole brain analyses, contrasts were calculated for each participant comparing the two rules, positions (inner vs. outer positions), responses (inner vs. outer responses) and colors (yellow vs. blue (rule 1) and pink vs. green (rule 2)). The contrasts for each participant were then entered into random effects analyses (one-sample *t*-tests).

Multi-voxel pattern analyses

Multi-voxel pattern analyses were carried out using MultiVariate Pattern Analysis in Python (PyMVPA) software (Hanke et al., 2008), in which support vector machine classification (Vapnik, 1995) is implemented by wrapping the LIBSVM library (Chih-Chung and Chih-Jen, 2001). We used a linear support vector machine, LinearCSVMC (http://

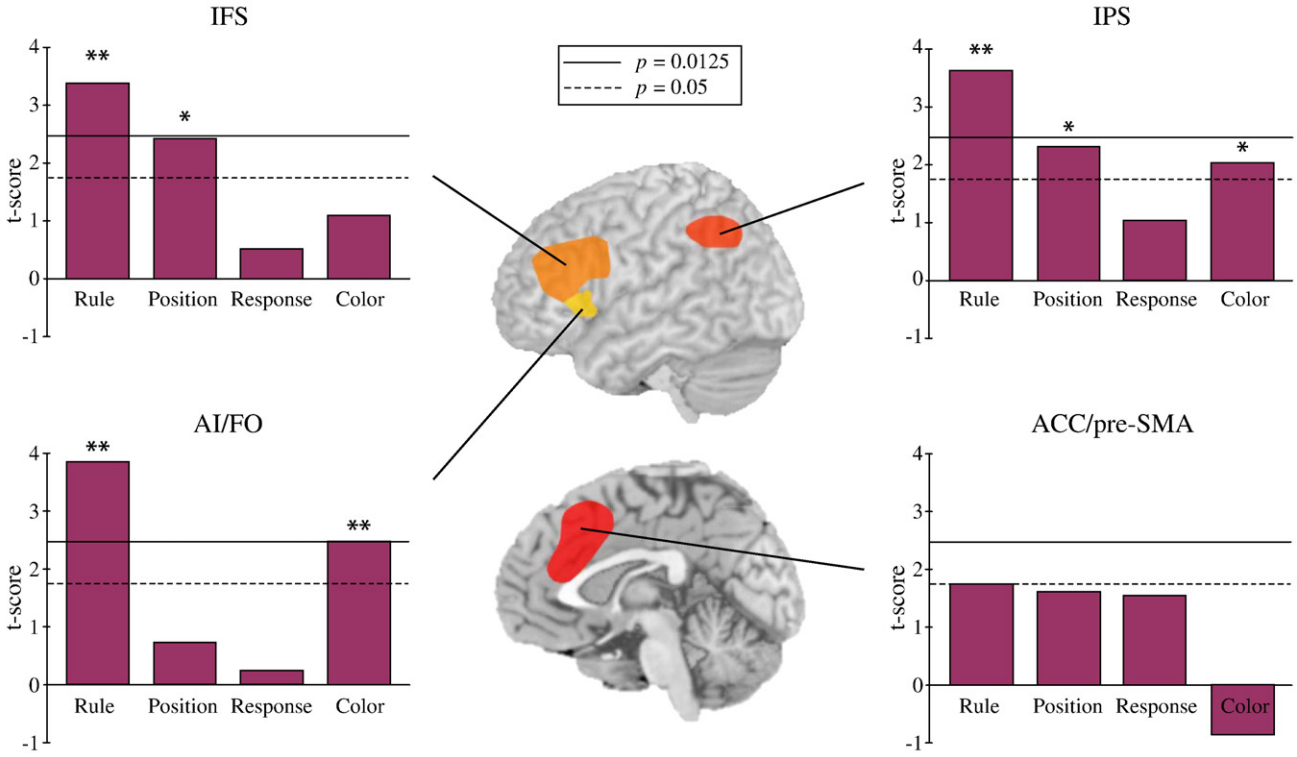

Fig. 2. Coding of rule, position, response and color in the MD ROIs. Bars represent *t*-score on a one-sample *t*-test of classification accuracy against chance. A score of 0 indicates chance level classification and positive values indicate above chance classification. Dotted line: significance threshold $p = 0.05$; solid line: significance threshold corresponding to Bonferroni-corrected *p*-value of 0.0125. $^{*}p < 0.05$, $^{**}p < 0.0125$.

www.pymvpa.org/api/mvpa.clfs.svm.LinearCSVMC-class.html). Beta estimation and second level random effects analyses were carried out using SPM5 (Wellcome Department of Imaging Neuroscience, London, UK; www.fil.ion.ucl.ac.uk).

Pattern analyses were carried out on ROI and whole brain bases. The ROI analysis allowed us to directly test our hypothesis that the MD regions code task-relevant information and events. The whole brain analysis allowed us to identify any additional feature coding outside of the MD system. For both analyses, 120 beta images (four stimulus positions, four responses and four background colors in each of ten blocks) were estimated for each participant with block and run means included as covariates of no interest. As in univariate analysis, each trial was modeled as an epoch lasting from stimulus onset until response, and each trial contributed to the estimation of three betas. Error trials were excluded.

The ROI analysis of rule proceeded as follows. For each participant, the eleven ROIs were deformed by applying the inverse of the participant's normalization parameters. This allowed us to carry out pattern classification analysis directly on the un-normalized data for each participant. First, classification of rule was carried out separately for each participant. For a given ROI, the pattern of beta values across the relevant voxels was extracted from each of the 40 relevant beta images (four color betas*10 blocks), yielding 40 multi-voxel vectors. 100% of the voxels in each ROI contributed to each vector, without feature selection. The linear support vector machine was trained to discriminate between the vectors pertaining to rule one and those pertaining to rule two. We used a leave-one-out ten-fold splitter: the classifier was trained using the data from nine of the ten blocks, and was subsequently tested on its accuracy at classifying the unseen data from the remaining block. This process was carried out in ten iterations, using all ten possible combinations of train and test blocks. The classification accuracies from the ten iterations were then averaged to give a mean accuracy score for that participant.

The mean classification accuracy for each participant was then entered into a second level analysis analogous to the univariate analyses described above. In the IFS, AI/FO and IPS ROIs, data were averaged across hemisphere and entered into a one-sample *t*-test against the classification accuracy expected by chance (50%). Paired *t*-tests examined any difference in coding accuracy between hemispheres. Where differences were found, post-hoc one-sample *t*-tests against chance were carried out for each hemisphere separately. A one-sample *t*-test against chance was also used for the single ACC/pre-SMA ROI. All tests against chance were one-tailed. We used a Bonferroni adjusted significance threshold ($p = 0.0125$) to account for the four MD regions tested.

The pipeline for the analyses of position and response was identical to that for rule. The color analysis was similar, except that classification of color was carried out within each rule separately. Mean classification accuracy for color in rules one and two was then entered into the second level analysis described above.

For regions where rule coding was statistically significant, a further analysis was included to eliminate the contribution of color coding to rule classification. Since rule was indicated by background color, it was possible that discrimination of color might drive discrimination of rule. To rule out this interpretation, we analyzed whether the rule discrimination generalized across the pairs of colors. That is, we trained the classifier to discriminate the two rules one using one set of colors (e.g. blue (rule one) vs. pink (rule two)) and tested the classifier on its prediction of rule using the other set of colors (e.g. yellow (rule one) vs. green (rule two)). This analysis followed the procedure outlined above except that in this case, a two-fold splitter (color set one vs. color set two) was used.

Finally, we compared the strength of rule coding to the other task features in a series of two-way ANOVAs with factors task feature (e.g. rule and position) and ROI (IFS, AI/FO, IPS, and ACC/pre-SMA; data for the first 3 averaged across hemispheres).

In order to identify any additional regions coding task-relevant information, whole brain pattern classification was carried out using a roaming spotlight (Kriegeskorte et al., 2006). For each participant, data were extracted from a spherical ROI (radius 5 mm) centered in turn on each voxel in the brain. A linear support vector machine was trained and tested as before, using data from each sphere, and the classification accuracy value for that sphere was assigned to the central voxel. This yielded whole brain classification accuracy maps for each individual for each of the five effects of interest outlined above. To combine data across individuals, classification accuracy maps were normalized by applying the normalization parameters extracted at the pre-processing stage of the univariate analyses, and were subsequently smoothed using a 10 mm FWHM Gaussian kernel. These images were entered into a one-sample *t*-test to identify voxels where classification was significantly above chance.

Results

Average accuracies and reaction times for different stimulus/response pairs within each rule are shown in Table 1. Overall participants performed with a high degree of accuracy ($M = 97\%$, $SD = 0.02$). There were no differences in accuracy rates between the two rules or between the inner and outer responses, but participants were more accurate in responding to the outer stimulus positions compared to the inner positions ($t(16) = 3.09$, $p < 0.01$). Reactions times were shorter in rule 1 compared to rule 2 ($t(16) = 3.84$, $p < 0.01$), for outer compared to inner stimulus positions ($t(16) = 6.05$, $p < 0.01$), and for outer compared to inner responses ($t(16) = 2.74$, $p < 0.05$). On average participants completed a total of 931 trials ($SD = 69.1$) across the ten task blocks.

Univariate analyses

In MD ROIs, no main effects of rule, position, response or color reached Bonferroni-corrected significance (Table 2). Sub threshold trends were seen for rule in the IPS ($F(1, 16) = 2.47$, $p < 0.05$), position in the AI/FO ($F(1, 16) = 6.97$, $p < 0.05$), response in the IFS ($F(1, 16) = 4.58$, $p < 0.05$) and color within rule one in the AI/FO ($F(1, 16) = 6.06$, $p < 0.05$). There was a significant main effect of hemisphere in the IPS in the color contrast for rule 2 ($F(1, 16) = 12.86$, $p < 0.0125$), reflecting increased activation in the left compared to right IPS.

In BA 17/18 there were no significant main effects of task feature. Activation tended to be greater in the left hemisphere, reflected by a main effect of hemisphere in the ANOVA with rule ($F(1, 16) = 5.41$, $p < 0.05$), response ($F(1, 16) = 5.44$, $p < 0.05$) position ($F(1, 16) = 5.45$, $p < 0.05$) and color in rule 1 ($F(1, 16) = 4.73$, $p < 0.05$). There were no significant task feature by hemisphere interactions. In BA 4 there were no significant effects.

In the whole brain analyses, no voxels survived FDR correction for any of the univariate contrasts (rule, position, response, color in rule 1, and color in rule 2).

ROI based pattern classification

MD regions

We predicted broad coding of task features in the MD regions and could assess differential coding of rule, position, response and color.

Table 1
Percent correct and reaction time data for the four stimulus positions and responses in rules 1 and 2.

	Rule 1				Rule 2			
Stimulus position	1	2	3	4	1	2	3	4
Response	2	1	4	3	4	3	2	1
Percent correct (%)	98	95	96	97	97	96	96	97
Reaction time (ms)	795	825	820	804	817	905	905	805

Stimulus and response positions are numbered from left to right (e.g. far left is stimulus position 1).

Table 2
Activation (difference in percent signal change) and *F*-scores for univariate effects in the MD ROIs.

	IFS		AI/FO		IPS		ACC/pre-SMA	
	Activation	*F*	Activation	*F*	Activation	*F*	Activation	*F*
Rule	0.007	1.57	−0.002	0.07	0.015	2.47*	0.002	0.16
Position	0.009	2.09	0.015	6.97*	0.011	1.28	0.007	0.94
Response	0.010	4.58*	0.006	2.41	0.002	0.37	−0.001	0.03
Color (rule 1)	0.007	0.94	0.019	6.06*	0.011	1.21	0.008	1.07
Color (rule 2)	0.007	0.72	0.007	0.72	0.006	0.49	0.001	0.00

Except where indicated by a negative activation difference, there was more activation in rule 1 vs. rule 2, inner vs. outer positions, inner vs. outer responses, blue vs. yellow, and green vs. pink. *$p<0.05$; no effects reached Bonferroni-corrected significance.

For each region, Fig. 2 shows the coding of rule, position, response and color, averaged where appropriate across the two hemispheres. Data are presented as *t*-scores representing the reliability of above-chance feature classification, and the solid line indicates the Bonferroni adjusted significance threshold of $p=0.0125$. We report effects of p greater than 0.0125 but less than 0.05 as sub threshold.

In the IFS we found significant coding of rule ($t(16)=3.38, p<0.0125$, mean classification accuracy $M=56.2\%$), and sub threshold coding of position ($t(16)=2.42$, $p<0.05$, $M=54.7\%$). Response and color coding were not significant (response: $t(16)=0.52$, $p=0.31$, $M=51.2\%$; color: $t(16)=1.09$, $p=0.15$, $M=51.3\%$). Rule coding was significantly stronger in the left IFS ($t(16)=3.81$, $p<0.0125$). Separate *t*-tests in the left and right IFS revealed highly significant rule coding in the left IFS ($t(16)=4.69$, $p<0.001$, $M=59.3\%$), and a trend towards rule coding in the right IFS ($t(16)=1.52$, $p=0.07$, $M=53.1\%$). Response coding was also significantly stronger in the left compared to right IFS ($t(16)=3.61, p<0.0125$). Separate *t*-tests in the left and right IFS revealed sub threshold coding of response in the left IFS ($t(16)=1.90$, $p<0.05$, $M=55.0\%$) and not in the right IFS ($t(16)=-1.11$, $M=47.4\%$). There were no other hemisphere effects ($ps>0.39$).

The AI/FO showed significant coding of rule ($t(16)=3.85, p<0.0125$, $M=54.3\%$) and color within rule ($t(16)=2.48, p<0.0125$, $M=52.8\%$). There was no significant coding of position ($t(16)=0.73$, $p=0.24$, $M=51.4\%$) or response ($t(16)=0.25$, $p=0.40$, $M=50.4\%$), and no hemisphere effects ($ps>0.19$).

The IPS showed significant coding of rule ($t(16)=3.63, p<0.0125$, $M=56.5\%$), and sub threshold coding of position ($t(16)=2.32$, $p<0.05$, $M=55.7\%$) and color ($t_{16}=2.04, p<0.05$, $M=52.9\%$). Coding of response was not significant ($t(16)=1.03$, $p=0.16$, $M=51.9\%$), and there were no hemispheric differences ($ps>0.16$).

In the ACC/pre-SMA, coding of rule, position and response approached significance (rule: $t(16)=1.74$, $p=0.051$, $M=52.9\%$; position: $t(16)=1.60$, $p=0.06$, $M=53.8\%$; response: $t(16)=1.55$, $p=0.07$, $M=53.8\%$). There was no coding of color ($t(16)=-0.87$, $M=48.4\%$).

Regions showing significant coding of rule were subjected to a further analysis to rule out the contribution of color to rule coding (color cross-generalization analysis, see Materials and methods). Rule coding was confirmed to be independent of color coding in all three regions showing significant coding of rule: IFS ($t(16)=2.72, p<0.01$, $M=54.1\%$), AI/FO ($t(16)=3.41, p<0.01$, $M=53.5\%$) and IPS ($t(16)=1.84, p<0.05$, $M=53.5\%$).

We compared the strength of rule coding to the other task features in a series of two-way ANOVAs with factors task feature (e.g. rule and position) and ROI (IFS, AI/FO, IPS, and ACC/pre-SMA; data for the first 3 averaged across hemispheres). Two significant main effects of task feature indicated that the MD regions showed more coding of rule than response ($F_{(1,16)}=3.77$, $p<0.05$ one-tailed) and more coding of rule than color ($F_{(1,16)}=6.99, p<0.01$ one-tailed). There was no main effect of task feature for rule vs. position ($F_{(1,16)}=0.66$, $p=0.43$). A further comparison of rule and position, taking into account any hemispheric difference, had factors task feature (rule and position), ROI (IFS, AI/FO and IPS), and hemisphere (left and right). This revealed a task feature by hemisphere interaction ($F_{(1,16)}=8.25$, $p<0.05$). Coding of rule was significantly greater than coding of position in the left hemisphere ($F_{(1,16)}=7.42$, $p<0.01$ one-tailed), and not in the right hemisphere ($F_{(1,16)}=0.34$, $p=0.57$). None of the analyses showed any significant feature * region interactions (all $ps>0.17$).

Overall we saw a broad pattern of coding in the MD regions. Rule was the most strongly coded task feature (significant in three of the four MD regions, with a trend in the fourth), followed by color and position which each showed significant or sub threshold coding in two regions, and finally response, only showing sub threshold coding in the left IFS. Comparing across regions, the representation of information in the IFS and IPS was similar: rule was the most strongly represented feature in these regions followed by position, color and finally response. The AI/FO similarly showed numerically more coding of rule than any other task feature.

Motor cortex and visual cortex

The motor cortex showed significant coding of response ($t(16)=3.59, p<0.01$, $M=57.2\%$). No other task features were coded significantly, and there was no effect of hemisphere ($ps>0.21$).

The visual cortex showed significant coding of the visual features of the task: position ($t(16)=3.50, p<0.01, M=59.3\%$) and color ($t(16)=3.60, p<0.01, M=55.9\%$). Surprisingly, the visual cortex also showed significant coding of rule ($t(16)=5.38$, $p<0.01$, $M=61.9\%$) and response ($t(16)=2.59, p<0.01, M=56.3\%$). The cross-generalization analysis confirmed that rule coding was not driven by color coding ($t(16)=3.26, p<0.01$, $M=56.6\%$). There were no hemisphere effects ($ps>0.10$). An additional analysis in which the visual ROI was restricted to BA 17 showed similar results. In this ROI we found significant coding of all four task features (rule: $t(16)=5.43$, $p<0.001$, $M=62.6\%$; position: $t(16)=3.74$, $p<0.001$, $M=60.0\%$; response $t(16)=2.54$, $p<0.05, M=55.1\%$; color $t(16)=3.81, p<0.001, M=56.8\%$), significant cross-generalization of rule between colors ($t(16)=3.45$, $p<0.001$, $M=57.9\%$), and no hemisphere effects ($ps>0.16$).

Comparison of multi-voxel and univariate results

Comparison of Fig. 2 and Table 2 shows that the pattern of multi-voxel effects did not tend to follow the pattern of univariate trends. This suggests that the multi-voxel results did not depend only on univariate trends. A supplementary analysis was carried out to clarify, for each contrast, what proportion of the most discriminative voxels (defined as voxels showing a univariate *t*-score greater than 1.5 or less than −1.5) showed greater activation in the direction of the univariate trends. We reasoned that if a substantial proportion of the more discriminative voxels showed greater activation in the opposite direction to the univariate trend (e.g. more activation to rule 1 than rule 2) this would provide information to the multi-voxel classifier that would be averaged out in the univariate analysis. Broadly, a similar proportion of voxels was found at each end of the distribution (Supplementary Fig. 1). In the MD regions, the proportion of the most discriminative voxels showing a

preference in the direction of the univariate trend was 57.7% for rule, 60.5% for position, 56.2% for response and 54.1% for color.

Whole brain pattern classification

Whole brain MVPA analyses largely confirmed the ROI results (Fig. 3, Table 3). To allow direct comparison between results, whole brain analyses were thresholded at $p<0.001$ with an extent threshold of 100 voxels.

Rule coding was seen in an extensive region of the left lateral frontal surface incorporating parts of the AI, FO and IFS (BA 45/47/44/6), the right lateral frontal surface including right FO (BA 44), the ACC/pre-SMA (BA 24/6), the posterior parietal cortex in both hemispheres including the area around the IPS (BA 40/7), and the visual cortex (BA 17/18/19). Additional areas of rule coding were found in the right middle and superior and left inferior temporal lobe (BA 20/21/37/22). A broadly similar pattern was seen in the cross-generalization whole brain analysis (Supplementary Fig. 2).

Position coding (inner vs. outer position) was seen in the right visual cortex (BA 17/18/19), and in the right parietal cortex including the posterior IPS (BA 7). In the left hemisphere position coding was seen in the visual cortex (BA 18).

Response coding (inner vs. outer response) was seen in left and right motor, supplementary motor and somatosensory areas (BA 4/6/3), in the left superior parietal lobe (BA 7), and in the visual cortices (BA 17/18), particularly on the left.

Color coding was seen in the left visual cortex (BA 17/18), in the precuneus at the midline (BA 7) and in a small region of the right IPS (BA 7).

Discussion

In this study we used MVPA to investigate the brain's representation of different types of task-relevant information. Of particular interest was a network of frontal and parietal MD regions encompassing the dorsal and ventral prefrontal cortex (IFS, AI/FO), intraparietal sulcus (IPS) and the anterior cingulate/pre-supplementary motor area (ACC/pre-SMA). We predicted a broad representation of the different task features, and compared the representation of different task features across regions.

Across MD regions, stimulus–response mapping rule was the most prominently coded task feature, with significant coding in IFS, AI/FO and IPS, and an additional trend in the ACC/pre-SMA. In this experiment, color was the cue indicating which rule to apply, and significant color coding was seen in the AI/FO, with additional sub threshold coding in the IPS. Coding of particular stimuli and responses was weaker, with sub threshold stimulus position coding in the IFS and IPS, and sub threshold response coding only in the left IFS. Color information may have contributed to rule coding in the main analysis, but rule coding was still widespread in the color cross-generalization analysis. The results show strong MD coding of a general rule for transforming stimuli into responses, with weaker coding of specific stimulus–response instances.

A number of univariate fMRI studies implicate the lateral prefrontal cortex, IPS and ACC/pre-SMA in the learning, retrieval, maintenance and implementation of rules (MacDonald et al., 2000; Passingham et al., 2000; Brass and von Cramon, 2002, 2004; Bunge et al., 2002, 2003, 2005; Brass et al., 2003; Bunge, 2004; Cavina-Pratesi et al., 2006; Crone et al., 2006; Donohue et al., 2008). For example, one such study showed increased activation of lateral prefrontal cortex, pre-SMA, and inferior and superior parietal cortex when participants maintained a set of stimulus–response contingencies compared to when they maintained a simple response plan (Bunge et al., 2003). Electrophysiological studies in non-human primates also suggest that single frontal and parietal cells code task rules of various kinds (Hoshi et al., 1998; White and Wise, 1999; Asaad et al., 2000; Wallis et al., 2001; Wallis and Miller, 2003). For example, Asaad et al. (1998) found that the activity of 44% of prefrontal neurons reflected the current mapping between a visual cue and the appropriate response. The activity of single cells in the right posterior parietal cortex has also been shown to reflect preparation of different task rules (Stoet and Snyder, 2004, see also Gail and Andersen, 2006).

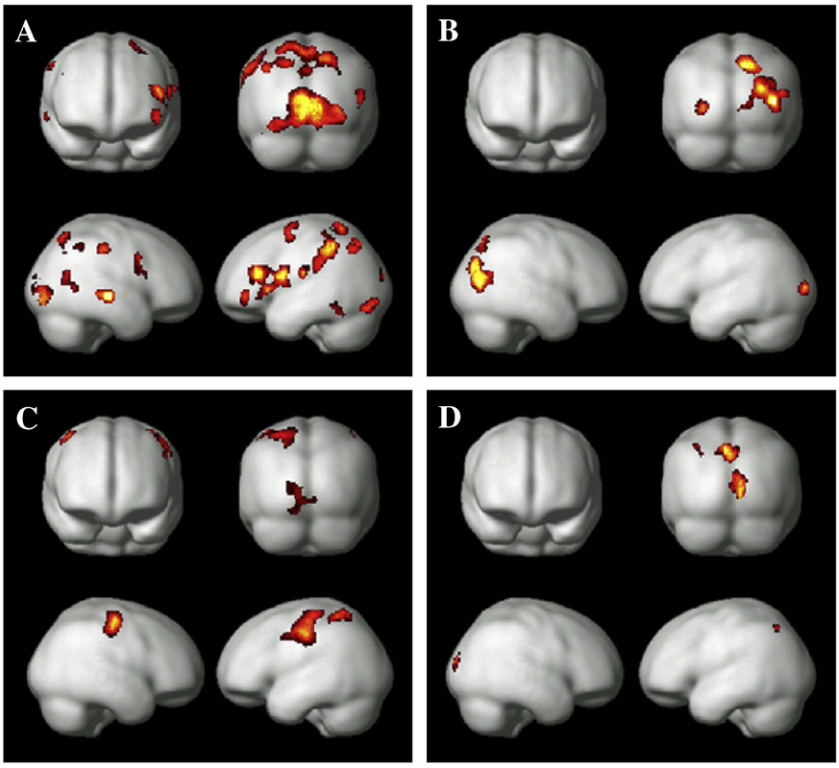

Fig. 3. Coding of (A) rule, (B) position, (C) response and (D) color in whole brain MVPA. To ease comparison between whole brain results for the four task features, results are thresholded at $p<0.001$ ($t=3.69$). The t-threshold for FDR correction would have been $t=2.50$ for rule, $t=4.54$ for position, and $t=3.75$ for response. No voxels survived FDR correction for color.

Table 3
Peak coding of rule, position, response and color in whole brain MVPA analyses.

Feature	Lobe	Cluster	Representative peaks					
			Hemisphere	Co-ordinates			Brodmann	Z-Score
				X	Y	Z	Area	
Rule	Frontal	Lateral frontal surface	Left	−52	4	14	6	4.83
			Left	−44	40	−2	47	4.06
			Left	−42	28	18	45	3.96
			Right	44	6	20	44	3.71
		Supplementary motor area	Right	4	−6	60	6	4.50
		Anterior insula	Left	−38	22	2		3.88
		Superior frontal lobe	Left	−22	−4	68	6	3.79
	Parietal	Inferior parietal lobe	Left	−52	−44	40	40	4.07
		Intraparietal sulcus	Right	28	−54	36	7	4.38
		Precuneus	Right	4	−54	58	5	3.98
		Superior parietal lobe	Left	−20	−54	66	5	3.73
			Left	−18	−68	48	7	3.36
		Postcentral gyrus	Left	−60	−32	30	2	3.66
			Right	54	−26	44	3	3.69
	Occipital	Visual cortex	Left	−18	−76	2	18	5.15
			Left	−28	−88	−12	18	4.04
			Right	6	−76	2	17	5.12
			Right	32	−84	−4	19	3.79
	Temporal	Superior temporal sulcus	Right	56	−22	−4	21	5.15
		Middle temporal gyrus	Right	56	−66	12	37	3.98
		Inferior temporal gyrus	Left	−46	−46	−14	20	4.55
Position	Occipitoparietal	Visual cortex	Left	−30	−96	4	18	3.86
			Right	30	−82	24	19	4.59
			Right	44	−78	10	19	4.24
		Precuneus	Right	16	−68	46	7	4.46
Response	Frontal	Precentral gyrus	Left	−36	−30	64	4	3.78
			Right	44	−20	50	4	5.10
		Supplementary motor area	Left	−4	−8	52	6	4.64
	Parietal	Postcentral gyrus	Left	−46	−20	40	3	4.30
		Superior parietal lobe	Left	−28	−50	60	7	4.13
	Occipital	Visual cortex	Left	−16	−84	8	17	3.61
			Left	−12	−80	−16	18	3.61
Color	Occipitoparietal	Early visual cortex	Right	10	−94	16	18	4.75
		Intraparietal sulcus	Left	−28	−60	38	7	3.84
		Precuneus	Left	−6	−66	46	7	3.88
			Right	2	−78	42	7	3.94

Results are thresholded at $p<0.001$, extent threshold = 100 voxels. Large continuous clusters are summarized by representative peaks.

Recent MVPA studies also implicate the MD regions in representing task sets (Hampton and O'Doherty, 2007; Soon et al., 2008; Bode and Haynes, 2009), For example Bode and Haynes (2009) showed discrimination of two stimulus–response mapping rules in the left IPS and ventral lateral prefrontal cortex. Here we extend this result to the bilateral MD network in a more complex stimulus–response mapping task and show that rule coding is abstracted across cues and across specific stimulus/response instances. Consistent with previous results, our data suggest that the pattern of activity in human frontoparietal cortex includes a strong representation of stimulus–response mapping rule.

The MD coding of stimulus identity in our data is also in keeping with numerous monkey studies showing position coding by individual prefrontal (Niki and Watanabe, 1976; Funahashi et al., 1989, 1993) and posterior parietal neurons (Andersen et al., 1985; Chafee et al., 2007). Response coding in the left IFS is also in line with data from individual prefrontal neurons (Sakagami and Niki, 1994; Hasegawa et al., 1998; Sakagami and Tsutsui, 1999).

For any multi-voxel discrimination, we might ask precisely what aspect of two events underlies that discrimination. In principal, the multi-voxel discrimination of rule, for example, could reflect coding of the exact stimulus–response mapping set, or could be based on discrimination of another feature such as transformation across the midline. In this study the two rules were well matched in several ways: both rules required spatial transformation between a set of four stimulus positions and a set of four finger responses, suppression of the dominant (spatially compatible) response tendency and orienting within the same set of spatial positions. Additionally our analyses demonstrate that discrimination of rule was not simply driven by differences in the background colors used to cue rule. Nonetheless, future studies will be needed to examine the precise factors that define rule representation.

In addition to the multi-voxel effects, there was an inconsistent pattern of univariate trends. In the case of rule coding, there was a trend towards more activation in rule 2 compared to rule 1 in the IPS region. This may have contributed to the rule coding seen in this region, since pattern analysis will also be sensitive to generalized univariate differences in activation. One interpretation of the univariate effect is that coding of rule is not only differential but also biased. At the single cell level, discrimination of a task feature is shown by a greater firing rate for one rule over another. If a population contains more cells with a preference for rule A over rule B, then the population code both discriminates and is biased towards one rule. Similarly in our study, the multi-voxel pattern of activation may both discriminate rule and show a bias towards a particular rule, leading to a univariate difference between rules when the response of a region is averaged across voxels. An alternative interpretation for the univariate difference is a generalized effect such as increased "effort" in rule two. Where both univariate and multivariate differences exist, it is not possible to determine whether the multi-voxel analysis discriminates the content of each rule or a more general property such as difficulty. That said, the univariate trends seen in our study were generally weak and inconsistent. Moreover, the profile of univariate trends (Table 2) did not tend to follow the pattern of multivariate effects (Fig. 2), and

the supplementary analysis suggested a substantial proportion of the most discriminative voxels showed a univariate difference in the opposite direction to the global univariate trend (Supplementary Fig. 1). For example, in the IPS, even though the average signal across the region was higher for rule 2 than rule 1, a large proportion of voxels showed the opposite pattern of activity, responding more strongly to rule 1 than rule 2. The pattern of results suggests that even in the regions where univariate trends were observed, the multivariate discriminations did not arise solely due to non-specific factors such as differences in task difficulty.

The visual cortex (BA 17/18) showed strong coding of the visual features of the task (position and color), as expected. Intriguingly, the visual cortex also showed representation of response and rule. This finding was manifest in both ROI and whole brain analyses, and remained present even when the visual ROI was restricted to BA 17. Our response analysis (inner vs. outer response) was not confounded with position, nor could it be driven by a generalized hemisphere effect due to the hand used to respond. One possibility is that this apparent response code reflects feedback from frontoparietal or motor areas. Interestingly, response coding has recently been seen in visual cortices in the macaque (Mirabella et al., 2007). In this data set, the firing rate of 29% of visually responsive cells in area V4 reflected which of two responses would be given. Similar considerations apply to the coding of rule. Since each rule was equally associated with each of the four positions and the four responses, coding of position or response alone could not drive the classification of rule. The cross-generalization analysis further confirmed that rule coding in this ROI was not driven by color coding. Intriguingly, Mirabella and colleagues (2007) also found evidence of rule coding in the visual cortex: the activity of 50% of visually responsive V4 cells recorded was modulated by which of two visual tasks the monkey was performing.

A possible issue arises for regions such as the visual cortex where coding of all three task features (position, rule and response) was seen. In our design, the combination of any two features also gives the third: the combination of position and rule information defines the required response, the combination of position and response defines the rule, and the combination of rule and response defines position. A general possibility is that classification of any one feature might be based on activity discriminating the other two, for example if unique patterns of activity were strongly driven by specific conjunctions of features (e.g. position 1 plus response 2). This is especially relevant for interpreting the pattern of effects in the visual cortex where all three task features were coded. Further work will be needed to assess the possibility of apparent coding of a third feature based on the combination of the other two.

In individual MD regions, we did not see simultaneous coding of all task features. However, our data do suggest that in some cases more than one task feature may be represented simultaneously. For example, the AI/FO showed both significant coding of color and significant cross-generalization across colors within the same rule. Given the relatively poor spatial resolution of fMRI, it is not possible to establish whether these features are coded by distinct neural populations, or whether the activity of overlapping populations of cells codes multiple stimulus features. In the visual system it has been suggested that information is represented on a columnar basis (Haynes and Rees, 2005; Kamitani and Tong, 2005), and a similar organization may also be present in the MD network. Conceivably, the extent to which cells with similar response profiles are clustered together will affect the extent to which fMRI is sensitive to the distinctions those cells code, perhaps contributing to differences in overall classification accuracies between brain regions. However, to be compatible with the role of these regions as multiple-demand processing areas, we would not expect the functional organization of the MD regions to be fixed. Rather we might speculate that the spatial organization of information in the MD regions would be flexible, adapting to represent the information relevant to the current task. The spatial origin of multi-voxel patterns in the MD regions provides an interesting avenue for further research.

In this study we have demonstrated multi-voxel representation of several task features in human frontoparietal cortex. The representation of multiple features was broadly spread across the MD regions, with strong representation of stimulus–response mapping rules and weaker representation of individual stimulus–response instances. The AI/FO coded rule and color, the IPS coded rule, color and position, and the IFS coded rule, position and (in the left hemisphere) response. Together the MD regions combine to represent all the task features needed to support appropriate behavior.

Acknowledgments

This work was funded by the Medical Research Council (UK) intramural program [U.1055.01.001.00001.01]. A.W. was supported by a Domestic Research Studentship/Millennium Scholarship funded by the University of Cambridge and the Newton Trust. We thank Matthew Brett for valuable help with analyses.

Appendix A. Supplementary data

Supplementary data associated with this article can be found, in the online version, at doi:10.1016/j.neuroimage.2010.04.035.

References

Andersen, R.A., Essick, G.K., Siegel, R.M., 1985. Encoding of spatial location by posterior parietal neurons. Science 230, 456–458.
Asaad, W.F., Rainer, G., Miller, E.K., 1998. Neural activity in the primate prefrontal cortex during associative learning. Neuron 21, 1399–1407.
Asaad, W.F., Rainer, G., Miller, E.K., 2000. Task-specific neural activity in the primate prefrontal cortex. J. Neurophysiol. 84, 451–459.
Bode, S., Haynes, J.D., 2009. Decoding sequential stages of task preparation in the human brain. Neuroimage 45, 606–613.
Brass, M., von Cramon, D.Y., 2002. The role of the frontal cortex in task preparation. Cereb. Cortex 12, 908–914.
Brass, M., von Cramon, D.Y., 2004. Decomposing components of task preparation with functional magnetic resonance imaging. J. Cogn. Neurosci. 16, 609–620.
Brass, M., Ruge, H., Meiran, N., Rubin, O., Koch, I., Zysset, S., Prinz, W., von Cramon, D.Y., 2003. When the same response has different meanings: recoding the response meaning in the lateral prefrontal cortex. Neuroimage 20, 1026–1031.
Brett, M., Anton, J.-L., Valabregue, R., Poline, J.-B., 2002. Region of interest analysis using an SPM toolbox [abstract]. 8th International Conference on Functional Mapping of the Human Brain. Sendai, Japan: NeuroImage, vol 16, No 2 (abstract 497).
Bunge, S.A., 2004. How we use rules to select actions: a review of evidence from cognitive neuroscience. Cogn. Affect. Behav. Neurosci. 4, 564–579.
Bunge, S.A., Hazeltine, E., Scanlon, M.D., Rosen, A.C., Gabrieli, J.D., 2002. Dissociable contributions of prefrontal and parietal cortices to response selection. Neuroimage 17, 1562–1571.
Bunge, S.A., Kahn, I., Wallis, J.D., Miller, E.K., Wagner, A.D., 2003. Neural circuits subserving the retrieval and maintenance of abstract rules. J. Neurophysiol. 90, 3419–3428.
Bunge, S.A., Wallis, J.D., Parker, A., Brass, M., Crone, E.A., Hoshi, E., Sakai, K., 2005. Neural circuitry underlying rule use in humans and nonhuman primates. J. Neurosci. 25, 10347–10350.
Cavina-Pratesi, C., Valyear, K.F., Culham, J.C., Kohler, S., Obhi, S.S., Marzi, C.A., Goodale, M.A., 2006. Dissociating arbitrary stimulus–response mapping from movement planning during preparatory period: evidence from event-related functional magnetic resonance imaging. J. Neurosci. 26, 2704–2713.
Chafee, M.V., Averbeck, B.B., Crowe, D.A., 2007. Representing spatial relationships in posterior parietal cortex: single neurons code object-referenced position. Cereb. Cortex 17, 2914–2932.
Chih-Chung, C., Chih-Jen, L., 2001. LIBSVM: A Library for Support Vector Machines. (Software available at http://www.csie.ntu.edu.tw/~cjlin/libsvm).
Crone, E.A., Wendelken, C., Donohue, S.E., Bunge, S.A., 2006. Neural evidence for dissociable components of task-switching. Cereb. Cortex 16, 475–486.
Cusack, R., Mitchell, D.J., Duncan, J., 2010. Discrete object representation, attention switching and task difficulty in the parietal lobe. J. Cogn. Neurosci. 22, 32–47.
Dehaene, S., Kerszberg, M., Changeux, J.P., 1998. A neuronal model of a global workspace in effortful cognitive tasks. Proc. Natl. Acad. Sci. U. S. A. 95, 14529–14534.
Desimone, R., Duncan, J., 1995. Neural mechanisms of selective visual attention. Annu. Rev. Neurosci. 18, 193–222.
Donohue, S.E., Wendelken, C., Bunge, S.A., 2008. Neural correlates of preparation for action selection as a function of specific task demands. J. Cogn. Neurosci. 20, 694–706.
Dosenbach, N.U., Visscher, K.M., Palmer, E.D., Miezin, F.M., Wenger, K.K., Kang, H.C., Burgund, E.D., Grimes, A.L., Schlaggar, B.L., Petersen, S.E., 2006. A core system for the implementation of task sets. Neuron 50, 799–812.
Duncan, J., 2006. EPS Mid-Career Award 2004: brain mechanisms of attention. Q. J. Exp. Psychol. (Colchester) 59, 2–27.
Duncan, J., Owen, A.M., 2000. Common regions of the human frontal lobe recruited by diverse cognitive demands. Trends Neurosci. 23, 475–483.

Funahashi, S., Bruce, C.J., Goldman-Rakic, P.S., 1989. Mnemonic coding of visual space in the monkey's dorsolateral prefrontal cortex. J. Neurophysiol. 61, 331–349.
Funahashi, S., Inoue, M., Kubota, K., 1993. Delay-related activity in the primate prefrontal cortex during sequential reaching tasks with delay. Neurosci. Res. 18, 171–175.
Gail, A., Andersen, R.A., 2006. Neural dynamics in monkey parietal reach region reflect context-specific sensorimotor transformations. J. Neurosci. 26, 9376–9384.
Hampton, A.N., O'Doherty, J.P., 2007. Decoding the neural substrates of reward-related decision making with functional MRI. Proc. Natl. Acad. Sci. U. S. A. 104, 1377–1382.
Hanke, M., Halchenko, Y.O., Sederberg, P.B., Hanson, S.J., Haxby, J.V., Pollmann, S., 2008. PyMVPA: A Python toolbox for Classifier-Based Data Analysis. German Society for Psychophysiology and its Application, Magdeburg.
Hasegawa, R., Sawaguchi, T., Kubota, K., 1998. Monkey prefrontal neuronal activity coding the forthcoming saccade in an oculomotor delayed matching-to-sample task. J. Neurophysiol. 79, 322–333.
Haynes, J.D., Rees, G., 2005. Predicting the orientation of invisible stimuli from activity in human primary visual cortex. Nat. Neurosci. 8, 686–691.
Haynes, J.D., Rees, G., 2006. Decoding mental states from brain activity in humans. Nat. Rev. Neurosci. 7, 523–534.
Haynes, J.D., Sakai, K., Rees, G., Gilbert, S., Frith, C., Passingham, R.E., 2007. Reading hidden intentions in the human brain. Curr. Biol. 17, 323–328.
Hoshi, E., Shima, K., Tanji, J., 1998. Task-dependent selectivity of movement-related neuronal activity in the primate prefrontal cortex. J. Neurophysiol. 80, 3392–3397.
Kamitani, Y., Tong, F., 2005. Decoding the visual and subjective contents of the human brain. Nat. Neurosci. 8, 679–685.
Kriegeskorte, N., Goebel, R., Bandettini, P., 2006. Information-based functional brain mapping. Proc. Natl. Acad. Sci. U. S. A. 103, 3863–3868.
Li, S., Ostwald, D., Giese, M., Kourtzi, Z., 2007. Flexible coding for categorical decisions in the human brain. J. Neurosci. 27, 12321–12330.
MacDonald III, A.W., Cohen, J.D., Stenger, V.A., Carter, C.S., 2000. Dissociating the role of the dorsolateral prefrontal and anterior cingulate cortex in cognitive control. Science 288, 1835–1838.
Miller, E.K., Cohen, J.D., 2001. An integrative theory of prefrontal cortex function. Annu. Rev. Neurosci. 24, 167–202.
Mirabella, G., Bertini, G., Samengo, I., Kilavik, B.E., Frilli, D., Della Libera, C., Chelazzi, L., 2007. Neurons in area V4 of the macaque translate attended visual features into behaviorally relevant categories. Neuron 54, 303–318.
Niki, H., Watanabe, M., 1976. Prefrontal unit activity and delayed response: relation to cue location versus direction of response. Brain Res. 105, 79–88.
Nyberg, L., Marklund, P., Persson, J., Cabeza, R., Forkstam, C., Petersson, K.M., Ingvar, M., 2003. Common prefrontal activations during working memory, episodic memory, and semantic memory. Neuropsychologia 41, 371–377.
Passingham, R.E., Toni, I., Rushworth, M.F.S., 2000. Specialisation within the prefrontal cortex: the ventral prefrontal cortex and associative learning. Exp. Brain Res. 133, 103–113.
Rorden, C., Brett, M., 2000. Stereotaxic display of brain lesions. Behav. Neurol. 12, 191–200.
Sakagami, M., Niki, H., 1994. Encoding of behavioral significance of visual stimuli by primate prefrontal neurons: relation to relevant task conditions. Exp. Brain Res. 97, 423–436.
Sakagami, M., Tsutsui, K., 1999. The hierarchical organization of decision making in the primate prefrontal cortex. Neurosci. Res. 34, 79–89.
Sigala, N., Kusunoki, M., Nimmo-Smith, I., Gaffan, D., Duncan, J., 2008. Hierarchical coding for sequential task events in the monkey prefrontal cortex. Proc. Natl. Acad. Sci. U. S. A. 105, 11969–11974.
Snyder, L.H., Batista, A.P., Andersen, R.A., 1997. Coding of intention in the posterior parietal cortex. Nature 386, 167–170.
Soon, C.S., Brass, M., Heinze, H.J., Haynes, J.D., 2008. Unconscious determinants of free decisions in the human brain. Nat. Neurosci. 11, 543–545.
Stoet, G., Snyder, L.H., 2004. Single neurons in posterior parietal cortex of monkeys encode cognitive set. Neuron 42, 1003–1012.
Vapnik, V., 1995. The Nature of Statistical Learning Theory. Springer, New York.
Wallis, J.D., Miller, E.K., 2003. From rule to response: neuronal processes in the premotor and prefrontal cortex. J. Neurophysiol. 90, 1790–1806.
Wallis, J.D., Anderson, K.C., Miller, E.K., 2001. Single neurons in prefrontal cortex encode abstract rules. Nature 411, 953–956.
White, I.M., Wise, S.P., 1999. Rule-dependent neuronal activity in the prefrontal cortex. Exp. Brain Res. 126, 315–335.